Beeswax-rosin mixtures in historical wet collection sealants: Qualitative analysis of their composition by DSC and ATR-FTIR spectroscopy

Baptiste Zuber, Sophie Cersoy, Marc Herbin, Michel Sablier, Véronique Rouchon

Vibrational Spectroscopy 117 (2021) 103310

Contents lists available at ScienceDirect

Vibrational Spectroscopy

journal homepage: www.elsevier.com/locate/vibspec

Beeswax-rosin mixtures in historical wet collection sealants: Qualitative analysis of their composition by DSC and ATR-FTIR spectroscopy

Baptiste Zuber [a], Sophie Cersoy [a,*], Marc Herbin [b,c], Michel Sablier [a], Véronique Rouchon [a]

[a] Centre de Recherche sur la Conservation (CRC), Sorbonne Université, Muséum national d'Histoire naturelle, Ministère de la Culture, CNRS, USR3224, CP21, 36 rue Geoffroy Saint-Hilaire, 75005, Paris, France
[b] Mécanismes adaptatifs & Evolution (MECADEV), Muséum national d'Histoire Naturelle, CNRS, Bâtiment d'Anatomie Comparée, 55 rue Buffon, Paris, 75005, France
[c] Direction des collections – Muséum national d'Histoire Naturelle, 57 rue Cuvier, Paris, France

ARTICLE INFO

Keywords:
ATR-FTIR
Py-GC/MS
DSC
Beeswax
Rosin
Wet collection

ABSTRACT

Wet collections sealants are historical materials that are essential for a sustainable preservation of specimens in fluid. Yet little is known about their composition, apart what can be found in technical records. Few scientific studies are dedicated to the identification of these materials that often correspond to complex mixtures. This work aims at facilitating the characterization of beeswax-rosin mixtures used for sealing wet collections. It explores the possibilities to quantify the proportions of beeswax-rosin mixtures by Differential Scanning Calorimetry (DSC) and Attenuated Total Reflectance Fourier Transformed mid-Infrared Spectroscopy (ATR-FTIR), two easy-to-run methodologies that require small samples. First these techniques were tested on model beeswax-rosin mixtures and appeared complementary. Then they were implemented on historical sealants and cross-checked with Pyrolysis Gaz Chromatography Mass Spectroscopy (Py-GC/MS) measurements, giving promising results. The impact, on the results, of ageing or of possible addition of third-party fatty materials such as animal fat or vegetal oil is also discussed.

1. Introduction

Zoological and medical collections serve as biological archives and store knowledge on the wide diversity of plants and animals. They are also precious testimonies on the past practices and works of naturalists. These items take multiples forms, from anatomical wax models to life-size taxidermy mounts, fossilized specimens, and injected organs. Among these, the preservation of specimens in fluids was widely used as it allows long-term safekeeping of internal organs and tissues (e.g. skin and muscles) while retaining the anatomical specificities of the specimen. However, it requires a constant attention from the conservators as, among other damages, the fluid may evaporate or oxidize thus endangering the specimens [1–5]. To limit these phenomena, a particular interest was paid in air-tight sealing techniques since the early XVIIIth century. The know-how of chemists and liquor-makers for chemical apparatus sealing were first adapted, then sealants were specifically developed for wet collections in order to limit as much as possible maintenance operations such as the refilling or replacement of fluids [2, 6]. These sealants correspond to pasty substances of variable colors and textures applied between the rim of the jar and the flat glass lid. Some of them came with one or several metallic foils and/ or bladders put over the lid and attached with a string under the jars rim. A few historical records and academic papers praise for the performance and durability of one or another type of sealant, but the archives regarding sealing operations are rather poor and do not cover the great variety of sealants observed today in collections [3,6–10].

Nowadays the jars are opened from time to time to consult the specimens, to optimize their conservation or to restore them. Re-sealing or re-conditioning appears then necessary. For this purpose, modern materials, such as silicones often replace original sealants. Also new gasket jars or pots with twist-off lids may be used. As these collections also belong to Heritage, these operations raise many questions regarding to the restitution of original materials. Improving knowledge on the history of preparation know-how and more specifically on the sealant's

Abbr$eviations: MNHN, Paris Natural History Museum; CAC, Comparative Anatomy Collection; BW beeswax, reference beeswax; CRC, Conservation Research Center (authors laboratory); RS rosin, reference rosin; TIC, Total Ionic Current; CBP, Calculated Beeswax Proportion; TBP, Tallow to Beeswax Proportion.

* Corresponding author at: CRC 36 rue Geoffroy-Saint-Hilaire, MNHN CP 21, 75005, Paris, France.
E-mail addresses: baptiste.zuber@edu.mnhn.fr (B. Zuber), sophie.cersoy@mnhn.fr (S. Cersoy), marc.herbin@mnhn.fr (M. Herbin), michel.sablier@mnhn.fr (M. Sablier), veronique.rouchon@mnhn.fr (V. Rouchon).

https://doi.org/10.1016/j.vibspec.2021.103310
Received 9 July 2021; Received in revised form 27 September 2021; Accepted 18 October 2021
Available online 20 October 2021

compositions would help to recognize effective ones and would be an aid to decision-making regarding management and reconditioning of fluid collections.

The work presented here is part of a larger study that aims to assess the diversity of historical sealants used at the Comparative Anatomy Collection (CAC) of the Museum national d'Histoire naturelle, Paris (MNHN). In 2017, a restoration campaign was launched in order to refill and maintain part of the wet collection. Together with posterior sampling, it gave the opportunity to establish a corpus of 66 sealants that were analyzed by Attenuated Total Reflectance Fourier Transformed mid-Infrared Spectroscopy (ATR-FTIR). This preliminary work led to the discrimination of seven composition groups in the corpus (unpublished results). Among these, a group of 4 samples seemed to be made up of beeswax-rosin mixtures.

The present work aims to go further in the characterization of this group and to define a methodology that would enable quantification of the beeswax-rosin proportions of the sealants present in the CAC. This does not only address the preliminary study samples but also a large part of the collection as this type of sealants was probably relatively common. It was indeed reported that mixtures of beeswax (60 %, w/w), rosin (35 %, w/w) and Meudon white (*Blanc de Meudon,* composed of calcium carbonate with clay) were used until the mid-1980s (personal communication with former collection assistant of the CAC). These mixtures have been since replaced by silicone-based sealants, but other institutions (e.g. the Bremmen Ubersee-Museum, Germany) still use them [11], which motivated the marketing of ready-to-use products.

These beeswax-rosin mixtures were also present in wet collections well before the XXth century: The Franklin Society of Providence (republished in [9]) praise a recipe that includes "Rosin, 2 part - Yellow Wax, 1 part – Red Ochres, or pounded brick, sufficient quantity to colour" [*sic*]; van Dam [3] reports the use of beeswax and rosin-based mixtures in historical Dutch sealants. François Peron, a French naturalist from the late XVIIIth century, describes the *lithocolle* (in text) recipe composed of beeswax, tar and turpentine oil with the addition of iron oxide [8]. This *"lithocolle"* aimed at providing a proper sealing for the jars submitted to the harsh condition of maritime transportation. Similar recipes can be found in other publications dedicated to natural history collections [10,11]. Sadly, all these sources lack of precision regarding proportions and preparation details. Defining an easy-to-run methodology to estimate beeswax-rosin proportions would help to document these aspects and estimate if there is a significant evolution of past practices from the early XIXth to the late XXth centuries.

The addition of fatty material into beeswax-rosin mixtures is also documented [10,12,13]. For example, a recipe of sealant composed of beeswax, rosin and stearin (7:3:1, w/w) was found in the Mycology collection of the university Claude Bernard (Lyon 1, France) (personal communication of Blandine Bärtschi - Curator of the mycological collections at Lyon 1, France).

This work also explores the possibilities offered by DSC and ATR-FTIR for the characterization of rosin-beeswax based sealants. ATR-FTIR and DSC measurements have been carried out on model samples consisting in beeswax-rosin mixtures of known composition, and eventually including some amount of tallow like substance. The impact of the model compositions on the ATR-FTIR and DSC signals have been evaluated, leading to calibration curves of ATR-FTIR and DSC response versus beeswax-rosin proportions. These calibrations were used to estimate the presence and proportions of beeswax and rosin in historical sealants. Pyrolysis Gas Chromatography / Mass Spectrometry (Py-GC/MS) have also been used to document more precisely the composition of the historical sealants. They will in addition help to evaluate the consistency of the ATR-FTIR and DSC approaches.

2. Materials and methods

2.1. Description of the samples

2.1.1. Beeswax and rosin pure compounds

The beeswax used in this study is a commercial product and will hereafter be referred as "BW beeswax". It is presented as pure beeswax and marketed for old-fashioned furniture polishing (Cire d'antiquaire Louis XIII, *Grande droguerie Lyonnaise*, Lyon, France). The possible presence of additives in this commercial product was researched by DSC, ATR-FTIR and Py-GC/MS but not found. All signatures are identical to those of a beehive fragment hereafter referred as "honeycomb fragment" originating from the CRC's natural product collection (laboratory label: "cire gauffrée 1997"). Therefore, the BW beeswax is considered in the following as pure beeswax.

The rosin used in this study was called "RS rosin" and corresponds to a full batch of resinous material found in the CAC and certainly used by a former curator. The rosin was kept away from heat and light and preserved in a cylindrical glass jar. It was analyzed by ATR-FTIR and Py-GC/MS and the resulting signatures were identical to those of a pure rosin samples from the CRC's natural products collection.

Finally, a ready-to-use beeswax-rosin mixture available on the market for sealing in wet collections was also selected (Bienenwachs-Kolophonium-Mischung, Bauer Handels GmbH, Fehraltorf, Switzerland) [14]. It was developed and tested by K. Wechsler, curator at the Bremen Ubersee museum [11]. The mixture is presented as 75 % beeswax and 25 % rosin by the provider and will hereafter be referred to as "Bauer mixture".

2.1.2. Fat additives

To produce beef tallow in a quick and cost-effective manner, beef fat tissues was purchased from the local butcher shop and submitted to a treatment inspired from the tallow rendering process used in the food industry: it was cut in small cubes and heated in a beaker at 80 °C during a few hours. Periodically, the clear yellow liquid oozing from the fat was collected. When stored in the fridge at 5 °C, it solidifies into a white greasy solid that was considered as model beef tallow.

2.1.3. Mixtures of model compounds

Model mixtures of beeswax and rosin have been made following a protocol inspired from *Gaillard et al.* [15]. Names and specifications of

Table 1
List of model mixtures. Mass proportions, heating temperature and duration are stated for each mixture for A and B series. The models marked with an asterisk correspond to mixtures that have presented problems in the solubilization of rosin.

Models	Beeswax Content α [%, w/w]	Rosin mass m_R [g]	Beeswax mass m_B [g]	Heating temperature T_H [°C]	Heating time t [min]
A_0	0	3	0	100	15
A_{10}	10.2	4.51	0.51	100	15
A_{15}	15.1	4.28	0.76	100	15
A_{20}	19.8	4.05	1.00	100	15
A_{25}	24.9	3.76	1.25	100	15
A_{40}	40.3	3.07	2.07	100	15
A_{60}	60.5	2.02	3.09	100	15
A_{75}	75.0	1.25	3.75	100	15
A_{80}	79.5	1.05	4.06	100	15
A_{85}	84.9	0.76	4.26	100	15
A_{90}	90.0	0.50	4.52	100	15
A_{100}	100	0	3	100	15
B_0	0	3	0	80	30
B_{20}*	19.9	3.99	.99	80	30
B_{40}*	40.2	3.02	2.03	80	30
B_{60}	60.0	2.03	3.04	80	30
B_{80}	79.9	1.01	4.02	80	30
B_{100}	100	0	3	80	30

each model mixture are available in Table 1. Two temperature values T_H were tested, leading to two series of models: 100 °C (A series) and 80 °C (B series). The beeswax was first melted at a temperature T_H in a sand bath. Crushed rosin was then gradually introduced. The complete dissolution of rosin was easily reached with the A series. With the B series, a layer of rosin appeared in the bottom of the beaker, which could not be completely solubilized by increasing the heating time. This effect was especially noticeable on B_{20} and B_{40} that are richer in rosin. The mixtures were kept under agitation at Th for 15 or 30 min (t) then let at ambient temperature to cool down. In addition, pure beeswax and rosin were submitted to the same treatments to evaluate the impact of heating on their thermal and spectral properties. These additional models are referred to as A_0, A_{100}, B_0 and B_{100} (Table 1).

Three additional models deviating from A_{75} have been prepared, replacing a fraction of the beeswax content with tallow. Proportions were chosen to reproduce tallow addition. Therefore 7.5, 18.75 and 37.5 % beef tallow (w/w) were introduced respectively corresponding to 10, 25 and 50 % of the beeswax mass. These additional models will be referred as A_{75_10}, A_{75_25} and A_{75_50}. Beef tallow was initially added to the beeswax before rosin addition, then the mixture was heated during 15 min at 100 °C, these models behave similarly to the A model series bar the fact that the more tallow they contain the softer they were.

2.1.4. Historical sealants from the MNHN

Four samples of sealant materials from the CAC were chosen in the framework of this study (see Table 2 and Appendix A). All related pieces have been restored and are now sealed with a silicon-based seals.

2.1.4.1. Sample A-11870. This sealant was a soft red paste collected from the lids of a jar (MNHN-ZM-AC-A11870, collection from the MNHN of Paris [16]) containing the lower jaw of a sperm whale (*Physeter macrocephalus*). The artefact is in the collection since the mid-19th century. However, there is no indication if the sealant is original or from a later restoration. The sample was collected in February 2019 and was chosen because of its appearance, suggesting a beeswax/rosin mixture. The lid of the jar was covered with a metallic grey painted bladder. Raman spectroscopy measurements performed on this sealant sample (see Appendix B) highlighted the presence of cinnabar as a red pigment (HgS, vermillion).

2.1.4.2. Sample A-4802. This brittle brown sample was collected during the 2017 restoration campaign. The jar (MNHN-ZM-AC-A4802, collection from the MNHN [17]) contained the brain of a male black bear (*Ursus americanus*) which died at the Paris MNHN's Menagerie in 1850. This item has been restored several times in the past as the conservative fluids is reported to have been changed. We may suppose that the sealant was made around 1887, since this date corresponds to its last mention in the inventory record [31].

Table 2
List of historical sealants collected on CAC artefacts with inventory numbers, names of species, date of entry, mentions of previous restorations in inventory records and description of visual aspect.

Inventory number	Specimen	Entrance in the collection	Last known restoration	Aspect
A-11870	Sperm whale (*Physeter macrocephalus*)	Mid-19th century	unknown	Red soft paste, came with a painted bladder
A-4802	Black bear (*Ursus americanus*)	1850	1887	Brittle brown seal
A-8407	Orangutan (*Simia satyrus*)	1892	unknown	red-brown paste came with a metallic foil
1930-151	Lemur (*Maki vari*)	1930	2017	Very brittle, black

2.1.4.3. Sample A-8407. This red sealant was collected during the 2017 restoration campaign on a jar (MNHN-ZM-AC-A8407, collection from the MNHN of Paris [18]) containing an orangutan brain (*Simia satyrus*). The primate comes from the Paris MNHN's Menagerie. It died in 1892 and was prepared during the same year. The specimen is in a poor condition (loss of coloration, and tissues darkening). This damage suggests that the specimen was exposed to an aggressive conservation fluid such as the Owen liquor. Yet the inventory records do not mention any restoration before 2017 and at this date, the conservative fluid was already formalin. The lid of the jar was covered with a metallic foil identified as tin by X-ray fluorescence analysis (unpublished results). The sealant is more brittle than the A-11870 sample and its red color is also attributable to the presence of cinnabar (confirmed by Raman spectroscopy, see Appendix B).

2.1.4.4. Sample 1930-151. This sealant comes from a jar (MNHN-ZM-AC-1930-151, collection from the MNHN of Paris [19]) containing the genital organs of a lemur (*Maki vari)*. According to the inventory records it entered the collection in 1930. Appearance-wise, this sample differs largely from the others as it is dark and brittle.

2.2. Instrumentation and methodology

2.2.1. Attenuated total reflexion – fourier transform infrared spectroscopy (ATR-FTIR)

ATR-FTIR measurements were carried out using an Alpha (Bruker) spectrometer equipped with a diamond ATR module. The spectra were recorded between 375 and 4000 cm^{-1}, with a resolution of 4 cm^{-1} and accumulating 120 scans. The signal was kept under a maximal absorption value of 0.3 in order to avoid any saturation issues. Background spectra were updated every three acquisitions for atmospheric correction. To evaluate the sample heterogeneity and other experimental variability sources (especially the variability associated with the contact between the sample and the ATR-crystal), three spectra were collected on each sample and treated separately.

The choice was made not to apply any ATR correction algorithms to our data as we cannot ensure that optical parameters of the mixtures are constant over the full range of composition. Indeed, such algorithms strongly depends on hard to evaluate parameters such as refractive indexes and penetration depth [20]. This consideration is in line with our willingness to keep mathematical transformation of the data to a minimum.

All ATR-FTIR spectra were submitted to a baseline correction consisting in six straight line segments, between points at 3997, 3658, 2196, 1974, 1530, 766 and 600 cm^{-1} (points were chosen as local minima of the sample spectrum, while avoiding points within the considered regions – except for the point at 1530 cm^{-1}). The second derivative of all acquired spectra have also being computed without baseline subtraction.

The data were then fitted in the chosen spectral region with the ATR-FTIR adjustment method described below.

2.2.2. Spectral adjustments

The FTIR signal of the beeswax/rosin mixtures was precisely investigated using the spectra of pure constituents and with an adjustment approach inspired from *Daher et al.* [21,22]. This approach relies on the spectral additivity hypothesis and supposes that the constituents of the mixture do not interact with each other in a manner that will strongly impact the spectrum of each constituent. It models the ATR-FTIR spectrum of a mixture $S_{mixture}$ with a linear combination of beeswax and rosin spectra as expressed mathematically here by:

$$S_{mixture} \approx \alpha_{BW} \cdot S_{BW} + \alpha_{RS} \cdot S_{RS} \quad (1)$$

Where S_{RS} and S_{BW} are respectively the reference spectra of pure rosin and beeswax, while α_{RS} and α_{BW} are respectively the beeswax and rosin associated coefficients. This adjustment was applied on restricted wavelength regions in which the FTIR spectra of beeswax and rosin showed specific features.

A Python script (see Appendix C) was written for the adjustment. The α_{BW} *and* α_{RS} coefficients were calculated using a conjugated gradient algorithm provided by the "optimize()" function of the ScyPy library [23]. The quality of the fit was estimated considering the R^2 coefficient of determination provided by the script. It was also checked with the calculation of the residual spectrum that corresponds to the difference between the measured and the fitted spectra.

$$Residual = S_{mixture} - (\alpha_{BW} \cdot S_{BW} + \alpha_{RS} \cdot S_{RS}) \quad (2)$$

Both approaches (R^2 and residual spectrum) enabled to estimate the spectral ranges that minimizes the deviation between the experimental and the model spectra.

As the previously introduced α weights are wavelength independent, the integration of relation (1) over the chosen wavelength region leads to the determination of characteristic band areas as a combination of those of pure products:

$$A_{mixture} \approx \alpha_{BW} A_{BW} + \alpha_{RS} \cdot A_{RS} \quad (3)$$

Where A_{BW}, A_{RS} and $A_{Mixture}$ are respectively the areas of pure beeswax, pure rosin, and fitted spectra in the considered wavelength region.

These areas are not only related to the amount of absorbent material in the mixture [21] but also to the experimental conditions of the acquisition. In order to remove the contribution of acquisition parameters, Eq. (3) is normalized with the total area of the fit $A_{Mixture}$:

$$1 \approx (\alpha_{BW} A_{BW} / A_{Mixture}) + (\alpha_{RS} A_{RS} / A_{Mixture}) \quad (4)$$

It leads to the determination of two coefficients C_{BW} and C_{BW} that are respectively related to the proportion of beeswax and rosin in the mixture.

$$C_{BW} = \alpha_{BW} A_{BW} / A_{Mixture} \text{ and } C_{RS} = \alpha_{RS} \cdot A_{RS} / A_{Mixture} \quad (5)$$

In order to perform the spectral adjustments in the region 2 - where the characteristic peaks at 1730 cm^{-1} and 1690 cm^{-1} tend to overlap, the same treatment have been realized using the second derivative of the considered spectrum $S_{Mixture}^{(2)}$. As expressed in the following equation:

$$S_{Mixture}^{(2)} \approx \beta_{BW} \cdot S_{BW}^{(2)}. + \beta_{RS} \cdot S_{RS}^{(2)}. \quad (6)$$

Where $S_{RS}^{(2)}$ and $S_{BW}^{(2)}$ are respectively the second derivative of the reference spectra of pure rosin and beeswax, while β_{RS} and β_{BW} are respectively the beeswax and rosin associated coefficients.

After calculation using the same Python script fed with the appropriated references, the β_{RS} and β_{BW} coefficients can be used to defined the contribution of each constituent $C_{BW}^{(2)}$ and $C_{RS}^{(2)}$ in the spectra's second derivative using the following relation:

$$C_{BW}^{(2)} = \beta_{BW} / (\beta_{BW} + \beta_{RS}) \text{ and } C_{RS}^{(2)} = \beta_{RS} / (\beta_{BW} + \beta_{RS}) \quad (7)$$

The beeswax coefficients C_{BW} and $C_{BW}^{(2)}$ of each model mixtures were plotted against known beeswax content thus providing calibration curves. These curves were used further on to estimate beeswax-rosin proportions on samples of unknown composition.

2.2.3. Differential scanning calorimetry (DSC)

DSC enables to measure the latent heat of a compound during a phase transition. The methodology of *Gaillard* et al. [15] was applied to measure the compounds proportions of a mixture, considering that the latent heat is the average of the pure compounds latent heats pondered by their relative proportions.

Thermograms have been acquired using a *DSC8000* (Perkin Elmer) apparatus. Indium (fusion temperature: 156.6 °C, Perkin Elmer) and dodecane (99 % purity, fusion temperature: -9.65 °C, Acros Organics) were used to calibrate the temperature and energy measurement. Between 1 and 2 mg of sample were introduced in a 20 µL aluminum capsule (Perkin Elmer), sealed and put into the calorimeter. A low sample weight was chosen to achieve analysis of historical materials available in small quantity. It also ensures that the capsule is submitted to a limited pressure during the experiment (thus minimizing the risk of opening). In order to maximize the contact area between the sample and the capsule, the sample were first melted down by a rapid heating (30 °C min^{-1}) up to 80 °C, then the samples were cooled down to 20 °C at 10 °C min^{-1} and finally heated back up to 80 °C at the same rate. Heat transfer is recorded only during the last two steps providing a solidification and a fusion profile for the sample. The heating speed of 10 °C min^{-1} was chosen because it offers the best signal to noise ratio. Baselines were subtracted from the thermograms using the *Origin Pro 8.5* software and choosing baseline points at fixed temperature for every curve (25, 70 and 80 °C for the fusion step and 21, 65 and 75 °C for the solidification step, using linear interpolation). Then the thermograms were divided by the sample weight and the heat flows (in mW•°C) were calculated by integration. The fusion heat flow (I_f) corresponds to the area of the fusion curve between 35 °C and 70 °C whereas the solidification heat flow (I_s) corresponds to the area of the solidification curve between 30 °C and 65 °C. It was found easier to consider a fixed integration domain that is larger than what is usually used for standard latent heat measurements [24]. This option enabled to include, for all samples, the full range of thermal events while keeping the same integration bound thus facilitating the data process. As discussed in Appendix D, it may introduce a small shift towards higher latent heat results, yet as every thermogram have been submitted to the same treatment, this shift was finally found has a negligible impact on the final result.

Finally, the fusion and solidification latent heats ΔH_f and ΔH_s of each sample were determined as follows:

$$\Delta H_f = K_T \cdot I_f \text{ and } \Delta H_s = K_T \cdot I_s \quad (6)$$

were K_T is a conversion constant equal to the inverse of the heating/cooling speed (here $K_T = 6$ s °C^{-1} as heating and cooling speed were set to 10 °C· min^{-1}).

Each model mixture and sealant sample have been analyzed 3 times in order to check reproducibility and evaluate the experimental dispersion. For each model mixture and sealant sample the mean of these three measurements was considered.

2.2.4. Pyrolysis gaz chromatography- mass spectrometry (Py-GC/MS)

The chromatograms have been acquired using a gas chromatograph (GC2010, Shimadzu) equipped with a column of dimension 30 m x0.25 mm x0.25 µm (ZB-5HT Zebron Inferno, Phenomenex) and coupled with a mass spectrometer (GC/MS Q2010 Plus, Shimadzu). Triplicates were recorded on all samples. For each analysis, approximately 30 µg of matter was introduced in a 50 µL stainless steel sample cup (Frontier Lab) with 2 µL of TMAH (25 % in methanol, Aldrich) and injected into the GC apparatus using a Py 2020iD Double Shot Pyrolyser (Frontier Lab) set at 600 °C.

The separation followed a protocol, already tested in our laboratory on sealants (unpublished results), that allows the detection of a large range of compounds including linear alkanes, methylated fatty acid and diterpenoids. The carrier gas was Helium (He ≥ 99,999 %, Alphagaz 1, Air Liquide). An injection split ratio of 1 over 90 was chosen. The temperature of the oven was kept at 40 °C for 8 min then increased up to 340 °C at a rate of 10 °C•min^{-1} for 30 min and finally the oven was allowed to stand at 340 °C for the last 10 min of the experiment (total time 48 min). The mass spectrometer was turned off during the first 18 min of experiment to avoid interference with TMAH related compounds. The Total Ionic Current (TIC) chromatograms were integrated in order to establish a peak list and the major compounds of each

samples were identified based on their retention time and mass spectra (by comparison with the NIST 11 mass spectral library).

The fours historical sealants described above and the BW/RS models and reference materials were submitted to Py-GC/MS to confirm their nature. The major peaks of each chromatogram were integrated and the area were normalized by the area of all considered peaks.

3. Results and discussion

3.1. Properties of pure compounds

Investigating beeswax-rosin mixtures necessitates having a good knowledge of the chemical compositions of individual compounds. Therefore, beeswax and rosin model compounds were characterized with the above-mentioned analytical tools. Their ATR-FTIR spectra and assignments are respectively reported on Fig. 1 and Table 3.

Chromatographic profiles can be found on Fig. 2. The most characteristic and easily detectable compounds were listed to facilitate identification of beeswax and rosin and their peak areas were plotted. These compounds correspond to linear alkanes (from C22 to C30), to methyl esters (C14, C15, C16, C16:1, C17, C18, C18:1 and from C24 to C30) and to the major diterpenoids methyl esters identified on the rosin reference (Table 4). All these compounds are not only specific markers of beeswax and rosin but also good indicators of other constituents such as paraffin or fatty material if they are present in significant amounts.

3.1.1. Beeswax

Beeswax is a complex mixture of organic compounds such as alkanes, esters and fatty acid. Its composition is relatively well known, and can be roughly described as a combination of odd-numbered alkanes, even-numbered fatty acid and long chain palmitic esters [25–28]. The Py-GC/MS analysis of the studied beeswax is in the line of these considerations (see Fig. 2).

On ATR-FTIR spectra, the large proportion of saturated aliphatic compounds is related to strong absorption peaks at 2955, 2916 and 2848 cm^{-1} and peaks of medium intensity at 1471, 1463, 728 and 718 cm^{-1} [36]. The beeswax IR spectrum is also presenting markers of free and esterified carboxylic function with an absorption band at 1730 cm^{-1} and an intense peak at 1170 cm^{-1} associated to the ester function stretching vibrations. The shouldering of the carbonyl band around 1710 cm^{-1} is one of the most specific features of the beeswax spectra: it makes it possible to distinguish beeswax from other materials, such as paraffin, and oils, that are also rich in saturated aliphatic compounds [29–31].

As discussed in the literature, the thermal properties of beeswax depend on the bee species who produced it. However, the production of different colonies of the same species have comparable latent heats [24, 32]. Our study deals with beeswax from European domestic honeybee (*Apis melifera*) meaning that the BW beeswax and the honeycomb fragment are expected to have a similar DSC response. This point was checked (Appendix D) and the values found for the fusion enthalpy (178 J/g, estimated between 39 °C and 67 °C) are consistent with published data [24]. In addition, it was shown (Appendix D and E) that the heating treatment has no significant impact on BW beeswax thermograms and ATR-FTIR spectra.

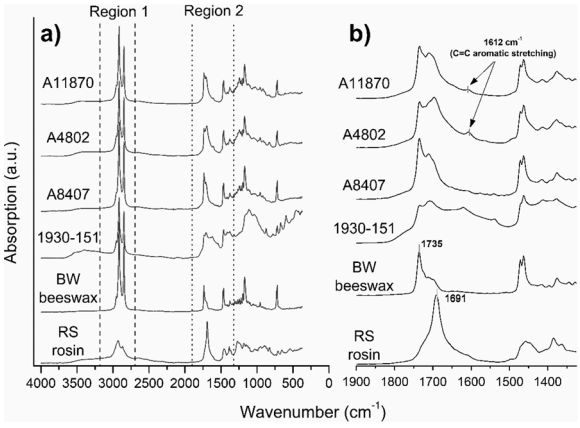

Fig. 1. IR spectra of rosin, beeswax, and historical sealants. a) full range spectra (4000 - 375 cm^{-1}). b) zoom on region 2 (1900 - 1325 cm^{-1}) showing specific signatures. From top to bottom: A-11870, A-4802, A-8407, 1930-151, pure BW beeswax, pure RS rosin.

Table 3
Assignment of rosin and beeswax ATR-FTIR absorption bands. The most specific features of each compound are underlined and bolded. The bands marked with an asterisk correspond to those that evolve during the aging of the material.

Wavenumber (cm^{-1})		Assignment
Beeswax	Rosin	
718		CH_2 rocking vibration (doublet in crystalline phases)
728		CH_2 rocking vibration (doublet in crystalline phases)
	882	=C—H deformation vibration
	896	C—C skeletal vibrations
	1108	C—C skeletal vibrations
	1130	C—C skeletal vibrations
	1151	C—C skeletal vibrations
1169		O—C=O asymmetric stretching vibration (ester)
1182		C—C skeletal vibrations
1243		C—O—C asymmetric stretching vibration (ester)
	1272	O—H deformation vibration (diterpenic acid)
	1385	C—H deformations vibration
	1457	C—H deformations vibration
1463		CH_3 asymmetric deformation vibration
1471		CH_2 scissoring vibration
1691		C=O stretching vibration (diterpenic acid)
1711		C=O stretching vibration (fatty acid)
1736		C=O stretching (ester)
2848		CH_2 symmetric stretching vibration
2867		C—H symmetric stretching vibration
2916		CH_2 asymmetric stretching vibration
2928		C—H asymmetric stretching (overlap of the different configuration)
2955		CH_3 asymmetric stretching vibration

3.1.2. Rosin

Rosin is obtained by selecting the heavier fraction of tree resin (mainly conifers) through a preparative distillation process. It is a complex mixture of diterpenoids compounds deviating from abietic acid [15,33]. Its diterpenoids distribution depends on the tree species, on the preparation process and also on the age of the sample. Indeed, unlike beeswax, resin is prone to oxidation causing the main constituent of historical rosin to be oxidized terpenes such as dehydroabietic acid [34]. For this study, the rosin reference was analyzed by Py-GC/MS after TMAH derivation. Nine predominant diterpenoids and their methyl ester derivatives were identified as rosin markers according to their mass spectroscopy [35,36] (see Table 4).

Among these compounds, the diterpenoids DT 5, DT 7, DT 8 and DT 9 are oxidized molecules that are formed during ageing [34,35]. The occurrence of such degraded compounds is consistent with the several decades of storage at ambient air conditions. However, RS rosin still contains relatively large amounts of DT1, DT 2, DT3, DT 4 and DT 6, which indicates that it is not fully oxidized. Even though the chromatographic data are very informative about its oxidation state, they do not allow the identification of the tree species nor the characterization of the fabrication process. Indeed, the accuracy of pyrolysis-chromatography is not sufficient to discriminate variations due to ageing from those due to origin (or processing in the case of real samples).

The rosin ATR-FTIR spectrum (See Fig. 1 and Table 3) is characterized by an intense and large absorption band around 1690 cm^{-1} that

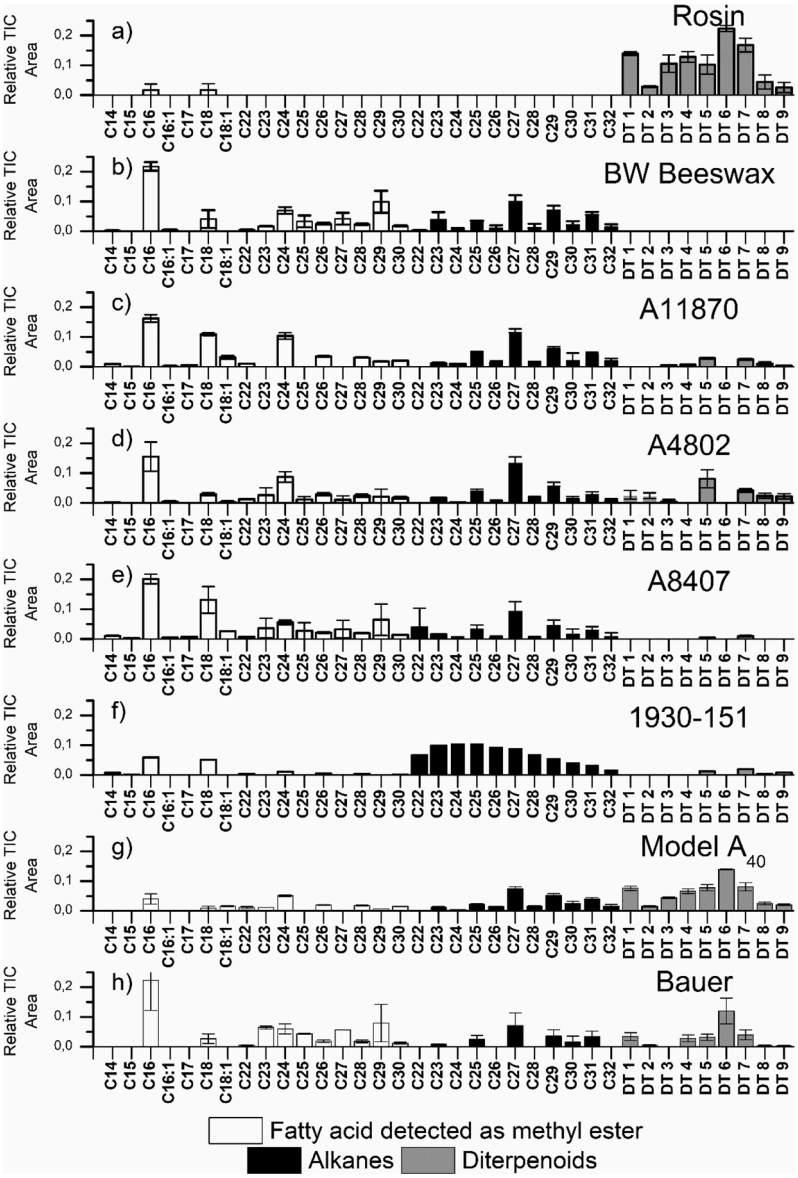

Fig. 2. Py-GC/MS composition profile of rosin, beeswax, model samples and historical sealants. The Total Ionic Current (TIC) area, normalized by the total area of the chromatogram, is plotted for each detected compound. White boxes: methyl ester; black boxes: alkanes; grey boxes: diterpenoids), error bars are representing the standard deviation.

Table 4
Identification of the major diterpenoids methyl ester found in reference rosin RS with their retention time (Ret. Time) in minutes and their relative TIC area expressed as an average of 3 measurements +/- standard deviation. Compounds marked with an asterisk correspond to oxidation markers of rosin.

Abbreviation	Compounds	Ret. time (min)	Relative TIC area proportion in RS rosin (% ± standard deviation.)
DT 1	methyl pimarate	29.5	14.6 ± 0.2
DT 2	methyl sandarocopimarate	29.9	3 ± 0.3
DT 3	methyl isopimarate	30.0	9.2 ± 0.2
DT 4	methyl palustrate	30.1	13.5 ± 2.4
DT 5	methyl dehydroabietate*	30.4	7.8 ± 6.9
DT 6	methyl abietate	30.8	23.5 ± 1.7
DT 7	methyl 7-hydroxyabietate*	31.2	17.7 ± 3.1
DT 8	methyl 3-hydroxydehydroabietate*	31.7	4.6 ± 2.3
DT 9	methyl 15-hydroxydehydroabietate*	31.9	2.6 ± 1.7

tends to enlarge with oxidation reactions taking place during ageing. Another distinctive feature of rosin lies in C—H vibration bands of medium intensity between 2928 cm^{-1} and 2867 cm^{-1} [30]. Although being less responsive in this area compared to beeswax, the rosin signal is significantly different from the beeswax signal allowing identification of rosin in a mixture. Beltran et al. [34] have reported the occurrence of a small absorption band around 1612 cm^{-1} which is related to rosin ageing and can be observed on some of our sample (see Fig. 1-a). This tend to support the presence of rosin in the studied sealants.

Rosin is an amorphous material [15] meaning its DSC curve is mostly flat in the considered temperature range as shown in the supplementary information (see Appendix F). Even though some thermal events occur [37], their enthalpies (≈5 J/g) are much smaller than those related to beeswax thermal events.

3.1.3. DSC and ATR-FTIR calibrations of beeswax-rosin mixtures

Constituting experimental data set from mixtures of known composition aimed at the construction of calibration curves that could be used for the analysis of historical samples of unknown composition. Both

solidification and fusion latent heats measured on the A and B series of beeswax-rosin mixtures were plotted versus known proportions of beeswax in the mixtures (Fig. 3). On the two A and B model series, the solidification and fusion latent heats measured on high beeswax content samples (above 50 %) are highly consistent. Conversely, some discrepancies are observed on low beeswax content mixtures (below 50 %), as the B sample series, heated at lower temperature, exhibits higher enthalpies than the A sample series. This underlines the fact that at low temperature beeswax and rosin are less miscible because of the rosin high viscosity. Therefore, the B model samples effectively contain less rosin than expected which led to an underestimation of their beeswax proportions, a point that is particularly noticeable for low beeswax proportions. For this reason, we decided to withdraw the B series points from the remainder of the work and to consider only the A series data for interpolation. As expected [15], the latent heat increases linearly with the beeswax content with a determination coefficient higher than 0.99. This demonstrates the possibility to quantify by DSC the beeswax-rosin ratio in mixtures of unknown proportions.

The ATR-FTIR response of beeswax and rosin compounds (Fig. 1) showed characteristic features between 3180 cm^{-1} and 2695 cm^{-1} (Region 1, C—H related bands) and between 1900 cm^{-1} and 1325 cm^{-1} (Region 2, C═O related band). These two regions were also chosen to test the ATR-FTIR adjustment methods described in section *2.2.2. Spectral Adjustment*.

The beeswax and rosin used to serve as reference correspond to samples A_{100} and A_0. They were thus submitted to the same thermal treatment as the considered mixtures. The adjustment method using baseline corrected spectra gave deceiving results on the A series in the region 2 related to C═O bands (see Appendix G and Appendix H). The poor interpolation comes from the overlapping of characteristic features of beeswax and rosin in this region of the spectrum. As a way to mitigate this effect the methodology using second derivative have been applied and yields more acceptable results.

In comparison, the region 1, characteristic of C—H vibrations, appears by far more suitable to model the mixture spectra as combinations of reference spectra. The adjustments are visually satisfactory (Fig. 4). They lead to determination coefficients R^2 values higher than 0.99 (appendix G) for the A series model. However, applying the method using the spectra second derivative in region 1 did not gave us as good

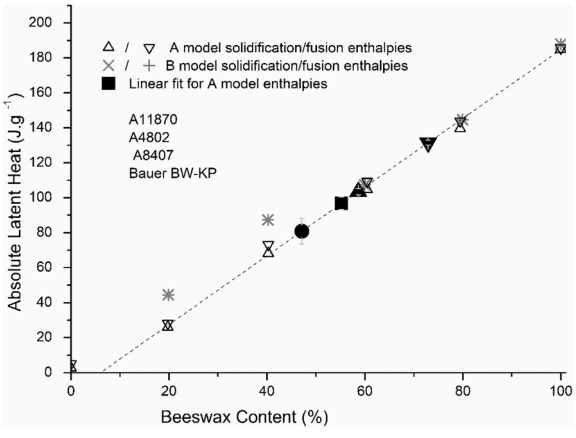

Fig. 3. DSC calibration curve. Absolute latent heats of model samples are shown versus beeswax contents. The A series data were linearly interpolated (dashed line, slope: 1.965 ± 0,021 $J{\cdot}g^{-1}{\cdot}\%^{-1}$, intercept: -11.74 ± 1.40 $J{\cdot}g^{-1}$, $R^2 = 0{,}99875$, 12 points) thus allowing the projection of the latent heat values of sealants of unknown composition on the plot. Empty triangles: A model series (upward: solidification, downward fusion), crosses: B model series (diagonal crosses: solidification, vertical crosses: fusion), filled square: A-11870; filled circle: A-4802, filled upward triangle: A-8407 and filled diamonds: Bauer commercial sample. Errors bars are representing standard deviation over 3 measurements.

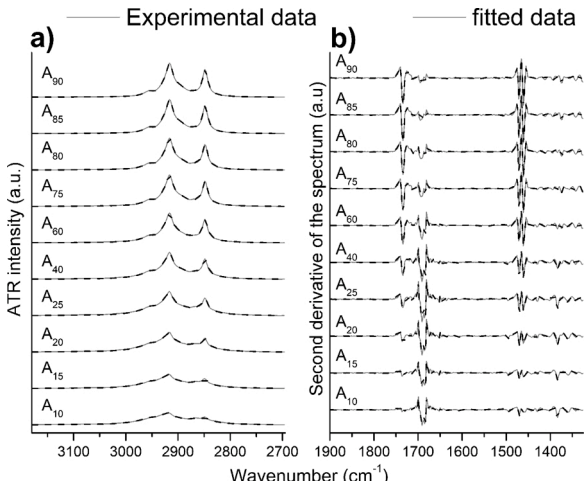

Fig. 4. ATR-FTIR spectra and spectral adjustments of the A model series in region 1 (3180-2695 cm^{-1}) together with their residual spectra and the spectra of pure beeswax and rosin. a) adjustment on region 1 using baselined spectra; b) adjustment on region 2 using second derivative. Solid grey lines: A model's experimental spectra, dashed black lines: adjusted spectra.

results as shown in appendix G.

The C_{BW} coefficients obtained for region 1 were plotted versus known composition, thus giving a calibration curve with a linear aspect between 25 % and 100 % beeswax content. As this range seems to be representative of the sealants' compositions, that all include a high proportion of beeswax, we considered a linear interpolation between 25 % and 100 % as a suitable calibration (Fig. 5).

The $C_{BW}^{(2)}$ coefficients calculated using the second spectra derivatives in region 2 were also plotted versus known composition (see Fig. 5). However, the linearity of this calibration curve is not as verified as with non-derivative spectra in region 1. Therefore, linear regression

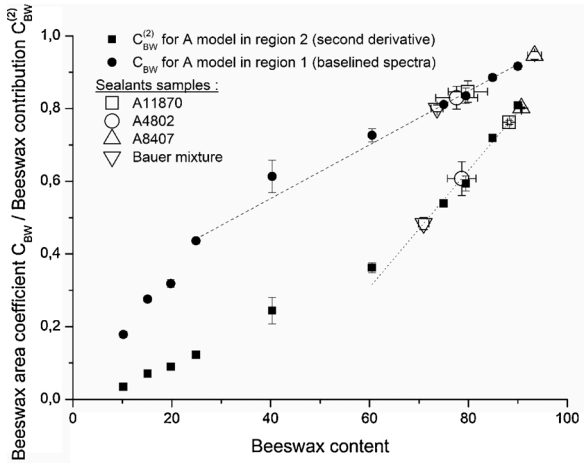

Fig. 5. Beeswax area coefficients C_{BW} in region 1 and beeswax contribution $C_{BW}^{(2)}$ in region 2 of the A series obtained in region 1 (3180-2695 cm^{-1}). The C_{BW} data for region 1 were linearly interpolated (black dashed line, slope: $7.38{\cdot}10^{-3}$ ± $0.15{\cdot}10^{-3}$ $\%^{-1}$, intercept: 0.257 ± 0.012, $R^2 = 0.99739$) between 25 % and 100 % beeswax contents (7 points). The $C_{BW}^{(2)}$ data for region 2 were linearly interpolated (black dotted line, slope: $1.61{\cdot}10^{-2} \pm 0.14{\cdot}10^{-2}$ $\%^{-1}$, intercept: -0.66 ± 0.12, $R^2 = 0.97142$) between 60 % and 100 % beeswax contents (5 points). The values obtained for sealants of unknown composition were projected on the plot. Empty diamonds: A models in region 1; empty squares: A model in region 2; filled square: A-11870; filled circle: A-4802; upward triangle: A-8407; downward grey triangle: Bauer commercial sample. Error bars are representing standard deviation over 3 measurements.

was only performed for beeswax content above 60 %.

The relative linearity of the curves obtained as well as the good performance of the adjustment methodology ensure us that the spectral additivity hypothesis is at least partially verified in our this of work.

3.2. Determining the composition of historical sealants

3.2.1. Qualitative characterization of historical sealants

The historical sealant samples were chosen among a larger corpus because they had in common similar ATR-FTIR features that could possibly be attributed to beeswax-rosin mixtures. In particular, the samples A-11870, A-4802 and A-8407 present a similar shape of the C—H associated bands around 2900 cm^{-1} and of the carbonyl bands around 1700 cm^{-1} (Fig. 1).

Sample 1930-151 also have strong absorption bands in these regions, but it differed from the above three mentioned samples in that it also contains gypsum ($CaSO_4{\cdot}2H_2O$), attested by large bands around 1104 cm^{-1}, 3520 cm^{-1}, 3400 cm^{-1} and sharp peaks at 1680 cm^{-1}, 1620 cm^{-1}, 670 cm^{-1} and 600 cm^{-1}). The occurrence of gypsum in the sample, in sufficient amount to be detected by ATR-FTIR jeopardizes any chance to determine a possible beeswax/rosin ratio through the DSC measurements: indeed, the presence of gypsum has a significant impact on the sample mass, leading to a systematic misevaluation of the organic part of the sample. In addition, the thermogram of sample 1930-151 (Appendix I) has a relatively different shape than those of beeswax-rosin mixtures (see Fig. 6). It is more congruent with the one of paraffin wax with a shift in temperature which could be attributed to the dependence of paraffin phase transition on its alkane distribution [38]. Py-GC/MS confirmed the occurrence of paraffin wax in sample 1930-151: the chromatographic profile (Fig. 2-f) exhibits neither the alkanes profile, nor the methyl ester profile expected for beeswax. Instead the presence of all linear alkanes with a maximum at C24 indicates a hydrocarbon wax, i.e. paraffin [38]. Thus, the sample 1930-151 was not appropriate to test the relevance of above defined ATR-FTIR and DSC calibration curves.

Conversely, the DSC and chromatographic profiles of the other three sealants (Fig. 2-cde) exhibit common features compatible with occurrence of a beeswax-rosin mixture. GC–MS data showed a predominance of odd-numbered alkanes, with a maximum at C27, together with the predominance of even numbered fatty acid (observed as methyl ester because of the TMAH derivation), the more abundant being C24. These types of profile are in line with the beeswax reference (Fig. 2-b). In addition, diterpenoids are detected in samples A-11870 and A-4802 (Fig. 2-cd) indicating the presence of rosin. Interestingly, oxidized species (namely DT5 methyl dehydroabietate and DT 7 methyl 7-hydroxyabietate) are present in higher amounts in historical samples than in fresh rosin. This is consistent with the expected ageing process of rosin described by *Beltran et al.* [34], which results in a depletion of abietic acid in favor of more oxidized diterpenoids.

In sample A-8407, only two diterpenoids were detected, in small amounts, which questions the occurrence of rosin. However, these diterpenoids are among the more oxidized (namely DT5 - methyl dehydroabietate and DT7 - methyl 7-hydroxyabietate) which is in line with the expected ageing of the rosin constituents, and its fatty acid fraction is comparable with those of beeswax.

Finally, sealant samples A-11870 and A-8407 present an unexpected amount of unsaturated fatty acid (namely oleic acid C18:1) which could be coherent with the presence of a third-party fatty material such as grease or oil. However, available chromatographic data are not sufficient to clearly establish this point.

3.2.2. Applying DSC and ATR-FTIR calibration curves: possibilities and limitations

Applying DSC and FTIR calibration curves to dose relative amounts of beeswax and resin was first attempted on the Bauer sample. According to the provider, this sample contains only beeswax and rosin, which was in good agreement with Py GC/MS data (Fig. 2h). The measurement of the latent heat yields 72.9 ± 0.7 % whereas the ATR-FTIR spectral interpolations indicated a beeswax content of 73.6 ± 1.2 % and 70.9 ± 1.0 % for baselined spectra and second derivative respectively. These values are close, to each other, and to the provider specification (75 %), meaning that the two dosage approaches were working satisfactorily on “fresh” mixtures used as sealant, nowadays, in fluid collections.

Historical sealant samples were then analyzed. The FTIR adjustment performed satisfactorily in region 1 using baselined spectra and in region 2 using second derivative (with coefficients of determination superior to 0,99, see Fig. 7), leading to a first determination of beeswax contents (Table 5, left column). Thermograms exhibited a similar shape than the Bauer mixture (Fig. 6) and extracted latent heats led to a second determination of beeswax contents (Table 5, right column). Yet these

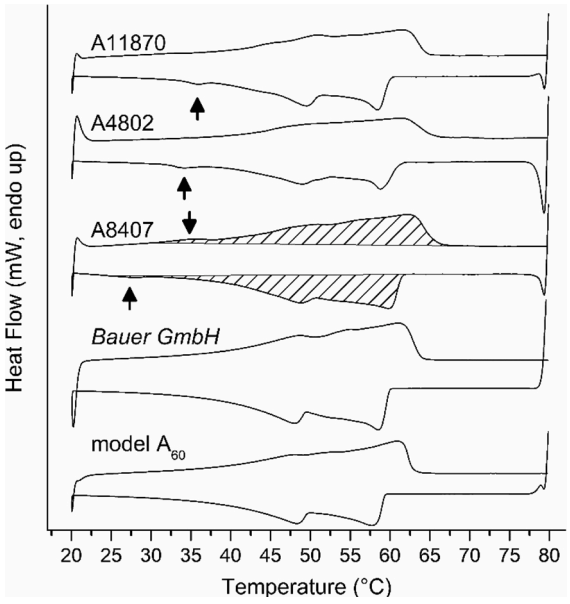

Fig. 6. Thermograms of the historical sealants, the Bauer mixture and the A_{60} model mixture. The hatched areas denote the integration domain for latent heat calculation. From top to bottom: sealant samples A-11870, A-4802 and A-8407, Bauer commercial sample, and model mixture A_{60}. Triangular arrows are denoting the thermogram features reported by Bartl et al. [40].

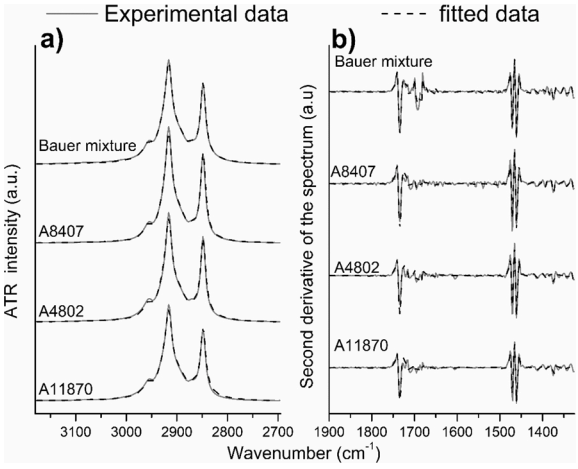

Fig. 7. ATR-FTIR and adjusted spectra of historical sealants and Bauer mixture. a) adjustment on region 1 using baselined spectra b) adjustment on region 2 using second derivative. Grey lines: experimental ATR-FTIR spectra, black dashed line: adjusted spectra.

Table 5
Estimated beeswax contents of historical sealants and Bauer mixture samples by FTIR and DSC considering the calibrations curves established on Figs. 5 and 3 respectively.

Sealants	ATR-FTIR		DSC
	Region 1 Baselined spectra	Region 2 s derivative	
A-11870	79.9 ± 4.0	88.2 ± 0.3 %	55.2 ± 1.8 %
A-4802	77.6 ± 4.2	78.6 ± 2.9 %	47.1 ± 3.7 %
A-8407	93.4 ± 1.4	90.7 ± 0.1 %	58.6 ± 0.9 %
Bauer mixture	73.6 ± 1.2	70.9 ± 1.0 %	72.9 ± 0.7 %

two sets of values (DSC and FTIR) differ significantly, the contents estimated by DSC being substantially lower than those determined by ATR-FTIR.

Several hypotheses may explain this lack of consistency. Among these, the ageing of the materials was first considered. Beeswax ageing modifies its latent heat due to the loss of lower weight alkenes and alkanes as reported by Bartl et al. [39]. A specific feature related to beeswax ageing, described by these authors [40], was observed on all thermograms (Fig. 6). It consists in a small peak around 30 °C, attributed to the partial segregation of lowest weight compounds of beeswax (mainly low molecular weight alkanes and alkenes). Yet this ageing cannot explain the gap between DSC and ATR-FTIR results, because it would lead to an increase of latent heat, and thus an over-estimation of beeswax contents, which is exactly the opposite of what is observed on the data (Table 5).

Presence of a third component is another possibility to account for the gap between DSC and ATR-FTIR results. Indeed, historical sealants might include some additives such as pigments. For instance, the samples A-8407 and A-11870 contained cinnabar (Appendix B). This red pigment being mostly thermally inert on the considered temperature range, its presence in these two samples mainly lead to an over-estimation of the thermally active mass, and thus to an under-estimation of the beeswax ratio [41]. In order to check the relevance of this hypothesis, the sealants A-8407 was dissolved in dichloromethane (a solvent which does not solubilize HgS). The dry residue mass after decantation was about 3 % of the initial mass, which is largely below the 33 % difference between DSC and ATR-FTIR results. Therefore, the pigment used to color the sealant cannot account for the gap between these estimations.

Another possibility lies in the addition of a third compound to the beeswax used for the sealants. Indeed, beeswax is an expensive material and was commonly blended with more affordable fatty materials such as beef tallow or paraffin [12,13,42]. Such practice has been reported in the field of fluid preservation [10]. As paraffin (that can be easily evidenced by Py-GC/MS) was not observed on samples A-11870, A-4802 and A-8407, we chose to investigate the impact of beef tallow addition on the measurement of beeswax contents by DSC and ATR-FTIR. The beeswax-tallow-resin mixtures (A_{75_10}, A_{75_25} and A_{75_50} model samples) were made for this purpose. They were softer than their corresponding beeswax-rosin mixture A_{75} (which could arguably make the sealant application and removal easier). As beef tallow is mostly inactive in the temperature range considered for DSC measurements, the replacement of beeswax by tallow tends to decrease the latent heat of the mixture. This is exactly what is observed on Fig. 8 on which Estimated Beeswax Proportion (EBP) determined by DSC decreases in the same proportions as known tallow to beeswax ratio (TBR) increases. This is consistent with the fact that tallow beef impacts the sample mass, but not the latent heat.

On the other hand, the fatty acids present in tallow contribute to the C—H absorption bands in region 1 in a similar manner than those of beeswax do. Therefore, the replacement of beeswax by tallow does not affect the ATR-FTIR response (Fig. 8) meaning that ATR-FTIR measurements are inappropriate to measure the beeswax proportions in

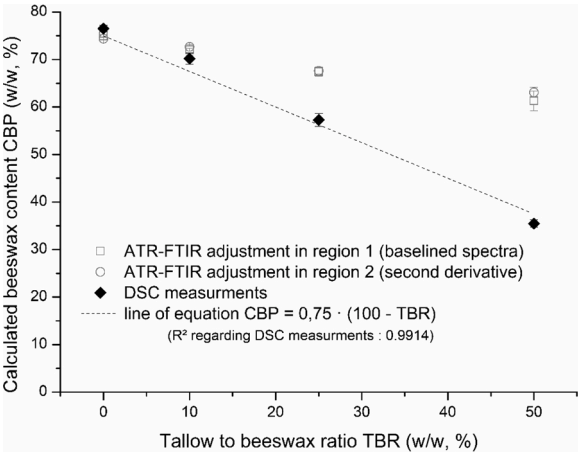

Fig. 8. Calculated beeswax proportion (CBP) via calibration curves versus tallow to beeswax ratio (TBR) for the model A_{75}, A_{75_10}, A_{75_25} and A_{75_50}. Grey diamonds: CBP using ATR-FTIR adjustment (R^2 values in grey) and calibration curve of Fig. 5; black squares: CBP using fusion enthalpy measurement and DSC calibration curve of Fig. 3, black circles: CBP using solidification enthalpy measurement and DSC calibration curve of Fig. 3. ATR-FTIR estimations do not depend on TBR values while DSC estimations decrease linearly with increasing TBR values (linear interpolation, black dashed line, equation CBP = 0.75·(100-TBR), $r^2 = 0.9914$). Error bars for the ATR-FTIR adjustments correspond to standard deviations over 3 measurements.

these systems but can instead be used to estimate the beeswax + tallow proportions.

Also, the discrepancies observed on historical sealants between ATR-FTIR and DSC estimations of beeswax contents probably mean that these sealants contain a third ingredient that has a substantial impact of ATR-FTIR spectra in the region of interest, but little impact on the latent heat measurements. The "low" estimation made with DSC measurements (Table 5, right column) is related to the actual beeswax proportions while the "high" estimation obtained with ATR-FTIR (Table 5, left column) would correspond to the proportion of beeswax and other fatty material in the whole system.

Supposing that this material corresponds to tallow, and that no other phenomenon interferes, the comparison of ATR-FTIR adjustments and DSC measurements makes it possible to quantify the beeswax blend. Reasoning this way with historical sealants drives us to conclude that our samples contained from one fourth to one third of non-beeswax fatty material (Table 6).

4. Conclusion

This work explores the possibility to use DSC and ATR-FTIR as easy-to-run methods for the characterization of sealants based on beeswax-rosin mixtures. These two techniques were first implemented on model mixtures prepared with varying proportions of beeswax.

DSC measurements enabled to estimate the fusion and solidification latent heats of the mixtures. Since rosin does not participate to phase transition in the considered temperature range, the latent heats were mostly related to the beeswax response and thus dependent on the beeswax proportions in the mixture. The DSC response is also highly specific of the presence of beeswax.

This is not the case of ATR-FTIR response that is largely impacted by

Table 6
Final estimated composition of the sealant samples.

Sealants	Final estimated composition (w/w)
A-11,870	57 % beeswax, 18 % fat and 25 % rosin. Trace amount of cinnabar.
A-4802	45 % beeswax, 20 % fat and 35 % rosin.
A-8407	57 % beeswax 28 % fat and 15 % rosin. Trace amount of cinnabar.

both beeswax and rosin. In the treatment of ATR-FTIR spectra, two regions of interest were chosen for spectral adjustments using combinations of pure components spectra. In the C—H related region (3180−2695 cm^{-1}), because of the more stable nature of the aliphatic fraction of the materials, these adjustments were of high quality and thus considered to establish a calibration curve for the quantification of beeswax proportions in unknown mixtures. Whereas because of the superposition of the most specific features of beeswax and rosin in this C═O related region (1900−1325 cm^{-1}) the second derivative had to be used in order to adequate adjustments. It was pointed out that the ATR-FTIR response gives information about the total aliphatic fraction of the sample and therefore could not spot beeswax only when this latter is blended with other aliphatic rich material such as grease or paraffin.

DSC and ATR-FTIR calibration curves were used successfully to quantify the composition of a modern sample made of beeswax and rosin (Bauer mixture). Values obtained with these approaches were highly consistent. Historical sealants from the CAC collection were thus further on considered. They were chosen for their ATR-FTIR spectral similarities with beeswax-rosin mixtures. They were also analyzed by Py-GC/MS to ensure their nature. One of them appeared to be composed of paraffin wax instead of beeswax and was therefore excluded from the study. The three other sealants, presenting a Py-GC/MS signal in consistent with rosin-beeswax mixtures, were analyzed by ATR-FTIR and DSC in order to assess their composition. Significant discrepancies were noticed between these two methods, the values obtained with ATR-FTIR being systematically above those obtained with DSC measurements.

These differences suggest occurrence, in the historical sealants, of a third-party compound, such as a fatty material with similar response to that of beeswax in the ATR-FTIR spectra. It was indeed common practice to blend beeswax with fat. Such a material is cheap and makes the mixture softer and probably easier to apply. The impact of the addition of some proportions of beef tallow was also evaluated on additional model samples, suggesting that the beeswax used in the historical sealants was probably blended with 30–50% fat material.

Author contributions

Baptiste Zuber: Conceptualization, Methodology, Investigation, Data curation, Software, Formal analysis, Visualization, Writing – Original draft preparation. **Sophie Cersoy**: Funding acquisition, Supervision, Writing – Review and Editing. **Marc Herbin**: Supervision, Resources (sealant samples), Writing – Review and Editing. **Michel Sablier**: Supervision, Resources (Py-GC/MS), Writing – Review and Editing. **Véronique Rouchon**: Supervision, Resources (DSC and FTIR), Writing – Review and Editing.

Funding

This project was supported by the Observatoire des patrimoines Sorbonne Université (OPUS) through a doctoral grant. Access to the collections was done in the framework of the RECOLNAT national Research Infrastructure.

Declaration of Competing Interest

The authors declare that they have no known competing financial interests or personal relationships that could have appeared to influence the work reported in this paper

Acknowledgments

The authors would like to acknowledge the support of Sylvie Heu and Yves Gaillard for her help with the DSC experiments as well as Celine Daher for allowing us to emulate her FTIR adjustment methodology and her precious advices. The sample selection came from data acquired by Eva Roussel and Elodie Bringer. This work also benefited greatly from the experience of Klaus Wechsler (preparator at the Überseemuseum, Bremen), Anja Friederichs (Conservator of the Arachnida and Myriapoda collection at the Museum für Naturkunde, Berlin) and Blandine Bärtschi (Curator of the mycological collections at Lyon 1, Lyon) on wet collections and sealing technics. We thank Céline Bens and Aurélie Verguin of the Collection de Pièces anatomiques en Fluides at the Muséum National d'Histoire Naturelle (MNHN) for their help.

Appendix A. Supplementary data

Supplementary material related to this article can be found, in the online version, at doi:https://doi.org/10.1016/j.vibspec.2021.103310.

References

[1] M. Herbin, ceroart (2013), https://doi.org/10.4000/ceroart.3432.
[2] J. Simmons, Fluid Preservation, A Coprehensive Reference, Rowman & Littlefield, 2014.
[3] A.-J. van Dam, Bulletin of the European Association of Museums of the History of Medical Sciences, Göteborg, Sweden, url:, 1997, pp. 22–28 http://www.eamhms.org/bulletin/eamhms_b23.pdf.
[4] A.-J. van Dam, Collect. Forum 14 (2000) 78–92.
[5] R. Waller, J. Simmons, Collect. Forum 18 (2003) 1–37.
[6] A. Pequignot, Ephaistos (2019), https://doi.org/10.4000/ephaistos.4563.
[7] J. Maissiat, Comptes Rendus Hebdomadaires Des Séances de l'Académie Des Sciences, Paris, url:, 1847, pp. 353–355 https://gallica.bnf.fr/ark:/12148/bpt6k29812/f353.image.r=Maissia.
[8] F. Péron, Voyage de decouvertes aux terres Australes pendant les annees 1800-1804 (continué par Louis Freycinet), Bertrand, url:, 1816 https://gallica.bnf.fr/ark:/12148/bpt6k74602q.
[9] United States Naval Lyceum, General directions for collecting and preserving articles in the various departments of natural history, J. Post (1834), https://doi.org/10.5962/bhl.title.100834 printer, New York, url:.
[10] M. Langeron, Précis de Microscopie, Masson&Cie, 1926.
[11] K. Anders-Grünewald, K. Wechsler, Der Präparator 46 (2000) 171–186.
[12] T.W. Cowan, Wax Craft, All About Beeswax. It's History, Production, Adulteration, and Commercial Value, S. Low, Marston&Co., Ltd., London, 1908.
[13] M. Maia, A. Barros, F.M. Nunes, Talanta 107 (2013) 74–80, https://doi.org/10.1016/j.talanta.2012.09.052.
[14] Bauer Handels GmbH, Taxidermy, 2021. Ch (2020), 2021-06-30, url: https://www.taxidermy.ch.
[15] Y. Gaillard, A. Mija, A. Burr, E. Darque-Ceretti, E. Felder, N. Sbirrazzuoli, Thermochim. Acta 521 (2011) 90–97, https://doi.org/10.1016/j.tca.2011.04.010.
[16] Specimen MNHN-ZM-AC-A11870, Muséum National d'Histoire Naturelle, Paris (France), Collection : Mammifères (ZM), 2021, 2021-06-30, url: http://coldb.mnhn.fr/catalognumber/mnhn/zm/ac-a11870.
[17] Specimen MNHN-ZM-AC-A4802, Muséum National d'Histoire Naturelle, Paris (France), Collection: Mammifères (ZM), 2021, 2021-06-30, url: http://coldb.mnhn.fr/catalognumber/mnhn/zm/ac-a4802.
[18] Specimen MNHN-ZM-AC-A8407, Muséum National d'Histoire Naturelle, Paris (France), Collection : Mammifères (ZM), 2021.
[19] Specimen MNHN-ZM-AC-1930-151, Muséum National d'Histoire Naturelle, Paris (France), Collection: Mammifères (ZM), 2021.
[20] S. Nunn, K. Nishikida, Application Note 50581: Advanced ATR Correction Algorithm, Thermo Fisher Scientific, 2008 url: https://assets.thermofisher.com/TFS-Assets/CAD/Application-Notes/D10241~.pdf.
[21] C. Daher, V. Pimenta, L. Bellot-Gurlet, Talanta 129 (2014) 336–345, https://doi.org/10.1016/j.talanta.2014.05.059.
[22] C. Daher, Analyse par spectroscopies Raman et infrarouge de matériaux naturels organiques issus d'objets du patrimoine: méthodologies et applications, Université Pierre et Marie Curie, 2012.
[23] P. Virtanen, R. Gommers, T.E. Oliphant, M. Haberland, T. Reddy, D. Cournapeau, E. Burovski, P. Peterson, W. Weckesser, J. Bright, S.J. van der Walt, M. Brett, J. Wilson, K.J. Millman, N. Mayorov, A.R.J. Nelson, E. Jones, R. Kern, E. Larson, C. J. Carey, I. Polat, Y. Feng, E.W. Moore, J. VanderPlas, D. Laxalde, J. Perktold, R. Cimrman, I. Henriksen, E.A. Quintero, C.R. Harris, A.M. Archibald, A.H. Ribeiro, F. Pedregosa, P. van Mulbregt, S. 1 0 contributors, Nat. Methods 17 (2020) 261–272, https://doi.org/10.1038/s41592-019-0686-2.
[24] R. Buchwald, M.D. Breed, A.R. Greenberg, J. Exp. Biol. 211 (2008) 121–127, https://doi.org/10.1242/jeb.007583.
[25] J.S. Mills, R. White, The Organic Chemistry of Museum Objects, second edition, Routledge, 1984 url: doi.org/10.1016/C2009-0-63247-5.
[26] I. Bonaduce, M.P. Colombini, J. Chromatogr. A 1028 (2004) 297–306, https://doi.org/10.1016/j.chroma.2003.11.086.
[27] A. Andreotti, I. Bonaduce, M.P. Colombini, G. Gautier, F. Modugno, E. Ribechini, Anal. Chem. 78 (2006) 4490–4500, https://doi.org/10.1021/ac0519615.
[28] E. Waś, T. Szczęsna, H. Rybak-Chmielewska, J. Apicult. Sci. 58 (2014) 99–106, https://doi.org/10.2478/jas-2014-0026.
[29] G. Socrates, Infrared and Raman Characteristic Group Frequencies: Tables and Charts, 3rd ed, Wiley, Chichester; New York, 2001.

[30] L. Svečnjak, L.A. Chesson, A. Gallina, M. Maia, M. Martinello, F. Mutinelli, M. N. Muz, F.M. Nunes, F. Saucy, B.J. Tipple, K. Wallner, E. Waś, T.A. Waters, J. Apic. Sci. 58 (2019) 1–108, https://doi.org/10.1080/00218839.2019.1571556.
[31] M. Regert, S. Colinart, L. Degrand, O. Decavallas, Archaeometry 43 (2003) 549–569, https://doi.org/10.1111/1475-4754.00036.
[32] R.G. Zhang, H. Zheng, H. Zhang, Y. Feng, K. Li, W.W. Zhang, Procedia Eng. 18 (2011) 101–106, https://doi.org/10.1016/j.proeng.2011.11.016.
[33] C. Azemard, M. Menager, C. Vieillescazes, Anal. Bioanal. Chem. 408 (2016) 6599–6612, https://doi.org/10.1007/s00216-016-9772-9.
[34] V. Beltran, N. Salvadó, S. Butí, T. Pradell, Anal. Bioanal. Chem. 408 (2016) 4073–4082, https://doi.org/10.1007/s00216-016-9496-x.
[35] J.M. Challinor, J. Anal. Appl. Pyrolysis 25 (1993) 349–360, https://doi.org/10.1016/0165-2370(93)80054-4.
[36] C.A. Genge, Anal. Chem. 31 (1959) 1750–1753, https://doi.org/10.1021/ac60155a016.
[37] R.G. Zhang, H. Zhang, Z. Zhang, H. Zheng, Y. Feng, W.W. Zhang, Adv. Mat. Res. 418–420 (2011) 643–650, https://doi.org/10.4028/www.scientific.net/AMR.418-420.643.
[38] V. Jayalakshmi, V. Selvavathi, M.S. Sekar, B. Sairam, Pet. Sci. Technol. 17 (1999) 843–856, https://doi.org/10.1080/10916469908949752.
[39] B. Bartl, M. Zapletal, S. Urbánek, M. Slavíková, J. Trejbal, Z. Hrdlička, Estud. Conserv. E Restauro 64 (2019) 138–145, https://doi.org/10.1080/00393630.2018.1544430.
[40] B. Bartl, J. Havlín, J. Trejbal, M. Ďurovič, Thermochim. Acta 566 (2013) 292–297, https://doi.org/10.1016/j.tca.2013.06.010.
[41] A. Burmester, Estud. Conserv. E Restauro 37 (1992) 73–81, https://doi.org/10.1179/sic.1992.37.2.73.
[42] L. Svečnjak, G. Baranović, M. Vinceković, S. Prđun, D. Bubalo, I.T. Gajger, J. Apic. Sci. 59 (2015) 37–49, https://doi.org/10.1515/jas-2015-0018.